Available online at www.sciencedirect.com

ScienceDirect

Energy Procedia 55 (2014) 179 – 185

Energy Procedia

4th International Conference on Silicon Photovoltaics, SiliconPV 2014

Comparison between Secondary Electron Microscopy Dopant Contrast Image (SEMDCI) and Electron Beam Induced Current (EBIC) for laser doping of crystalline silicon

Lujia Xu[a], Ziv Hameiri[b], Klaus Weber[a], Xinbo Yang[a,*]

[a]*Centre for Sustainable Energy Systems, Australian National University, Canberra, ACT 0200, Australia*
[b]*Solar Energy Research Institute of Singapore, National University of Singapore, 117574 Singapore*

Abstract

Laser doping of crystalline silicon has been the subject of intense research over the past decade, due to its potential to enable the fabrication of high efficiency and low-cost crystalline silicon solar cells. Information regarding the doping profile created by the process is critical for process optimisation, however is generally difficult to obtain. In this paper, a relatively new technique for characterising laser doping cross-sections — Secondary Electron Microscopy Dopant Contrast Image (SEMDCI) — is compared with the widely used Electron Beam Induced Current (EBIC) method. A good agreement between the two techniques regarding the p-n junction profile is demonstrated. The differences between the methods are attributed to the difference of the sensitivity. The comparison demonstrates the reliability and usefulness of the SEMDCI as a characterisation method for laser doping, which shows both the p-n junction outline and dopant distribution within the doped regions. The differences between the methods and the challenges associated with the application of the SEMDCI method are also discussed.

Peer-review under responsibility of the scientific committee of the SiliconPV 2014 conference

Keywords: SEMDCI; EBIC; laser doping

* Corresponding author. Tel.: +61 02 61250080; fax: +61 02 6125 0506.
E-mail address: lujia.xu@anu.edu.au

Peer-review under responsibility of the scientific committee of the SiliconPV 2014 conference
doi:10.1016/j.egypro.2014.08.112

1. Introduction

Laser doping offers an effective method to form heavily doped regions beneath the metal contacts of silicon solar cells. In this method the laser energy is used to selectively remove the anti-reflection coating (ARC) and passivation layers and simultaneously melt the silicon underneath to incorporate dopants into the melted volume, creating well defined heavily doped regions [1].

As the laser-doped junction depth and shape have a crucial impact on the performance of the solar cell, a method to measure them is required. A widely used method for this purpose is the Electron Beam Induced Current (EBIC) technique [1,2], which is based on collection of electrons in vicinity of the junction. When an electron beam, such as that in a Scanning Electron Microscope (SEM), strikes a semiconductor sample, it generates electron-hole pairs within the beam's interaction volume. If the sample contains a p-n junction and contacts, electron-hole pairs generated within a diffusion length from the junction may be collected, producing an electron beam induced current. In this case, the collected signal indicates the p-n junction location and can be superimposed on the SEM data to create an image. One of the main drawbacks of the EBIC technique is that it depends on the recombination rate at the surface where the beam impinges [3]. Another main limitation is that it only provides information on the location of the p-n junction but not on the dopant density profile. In addition, in most cases EBIC requires significant sample preparation, as well as electrical contacting in the microscope. Recently, a simpler and quicker technique for characterising laser doped cross-sections was developed, the secondary electron microscopy dopant contrast image (SEMDCI) [4,5]. SEMDCI is based on the observation that under certain imaging conditions, contrast is observed between differently doped semiconductor regions, where p-doped regions appear brighter than n-doped regions [6-12]. The contrast can be used to localise the p-n junction by a relatively abrupt change in dopant contrast and to image the dopant concentration distribution within the laser doped region.

In this paper, the SEMDCI and EBIC techniques are compared in order to evaluate the reliability and accuracy of the SEMDCI method. The comparison also highlights the advantages and the limitations of each of the techniques, so better use of them can be done.

2. Experimental

Boron and phosphorus spin-on-dopant (B-SOD/P-SOD) solutions, commercially available from Filmtronics Inc., were used as dopant sources. Single-side polished wafers with opposite dopant type to the SOD solution were chosen as substrates (see Table 1 for further details on the samples). Laser doping was achieved using a Diode Pumped Solid State (DPSS) laser operated in a pulsed mode with a repetition rate of 40 kHz. The spatial overlap between consecutive laser pulses was controlled by variation of the laser scanning speed. In SEMDCI, the p-n junction boundary of an n-type doped surface region is influenced by the p-type bulk doping concentration [4, 8, 13-15]. Therefore, both moderately and highly doped p-type substrates were used for the P-SOD samples. Samples were divided into three groups according the substrate polarity and resistivity. Within each group, three different scanning speeds were used (20 laser doped lines at each speed). In order to perform an accurate comparison between SEMDCI and EBIC, the laser doped lines were cleaved into two parts, one for SEMDCI and one for EBIC. In this way a direct comparison between the two sides of the same cross-section was possible. Since a freshly cleaved surface is preferred for SEMDCI, the SEMDCI measurements were preformed immediately after cleaving. From each group of lines, 2-3 cross sections with a good SEMDCI signal were chosen for further investigation by EBIC. The SEM equipment used for SEMDCI is Zeiss UltraPlus FESEM localized in the Centre for Advanced Microscopy, Australian National University, while the EBIC measurements were done using a DISS 5 EBIC from Point Electronic installed in Zeiss's Auriga 39-35 SEM at the Solar Energy Research Institute of Singapore (SERIS).

Table 1. Sample details

Sample ID	Substrate type	Substrate resistivity (Ω·cm)	Laser Power (W)	Laser scan speed (mm/s)	SEMDCI detectability	EBIC detectability
A1	P/Boron	1~10	0.7	5	Yes	Yes
A2	P/Boron	1~10	0.7	40	Yes (but very weak)	No
A3	P/Boron	1~10	0.9	200	Yes	Yes*
B1	P/Boron	0.01~0.05	0.7	5	Yes	Yes
B2	P/Boron	0.01~0.05	0.7	40	Yes	No
B3	P/Boron	0.01~0.05	0.9	200	Yes	Yes*
C1	N/Phosphorus	1~10	0.7	5	Yes	Yes
C2	N/Phosphorus	1~10	0.6	20	Yes	Yes
C3	N/Phosphorus	1~10	0.9	150	Yes	Yes

* Only some lines were detectable. Different cross-sections were used for the comparison

3. Result and analysis

3.1. Detectability

For each sample group, laser parameters and the detectability of the SEMDCI and the EBIC signals are listed in Table 1. As can be seen, with the exception of Sample A2 which was processed at low laser power and high scanning speed, the detected SEMDCI contrast was sufficient to allow characterisation with a reasonable signal to noise ratio. In contrast, several of the laser doped lines could not be characterised by EBIC. As EBIC requires a good electrical contact between the imaged area and the contact pad, samples with lowly doped lines or samples with discontinuous doping are not always suitable for EBIC measurement. Although this problem can be solved by metallisation of the doped line, it required an additional preparation, which complicates the sample preparation. As a contactless characterisation method, SEMDCI has an advantage over EBIC in this respect.

3.2. Agreement between the methods

Figure 1(a) is a representative example of a sample with good SEMDCI and EBIC signals. It demonstrates a good agreement between SEMDCI and EBIC in terms of the shape of the p-n junction boundary. Similar agreement was observed for most of the samples. These agreements indicate that SEMDCI can be used as a reliable technique for characterising of p-n junction, similar to the well-established EBIC method. Moreover, as shown in Fig. 1(b), a high contrast signal in SEMDCI likely corresponds to a high signal intensity in EBIC (compare the middle circled region in Fig. 1(b) with the two edge circled regions). This relationship is possible if the electric filed effect is taken into consideration. A possible mechanism of SEMDCI is the patch field effect, the stronger the patch field the higher the contrast observed in SEMDCI. The patch field strength is basically proportional to the built-in electric field of the p-n junction [15,16]. Therefore, if there is a strong built-in electric filed within the depletion region of the p-n junction that normally produces a high intensity EBIC signal, a corresponding strong patch field will result in a high contrast in SEMDCI. However, the signal generated by the EBIC technique is not only related to the electric field of the depletion region but also the surface recombination and bulk lifetime, which might partially explain the disagreement between SEMDCI contrast and EBIC signal intensity within the middle circled region in Fig. 1 (b).

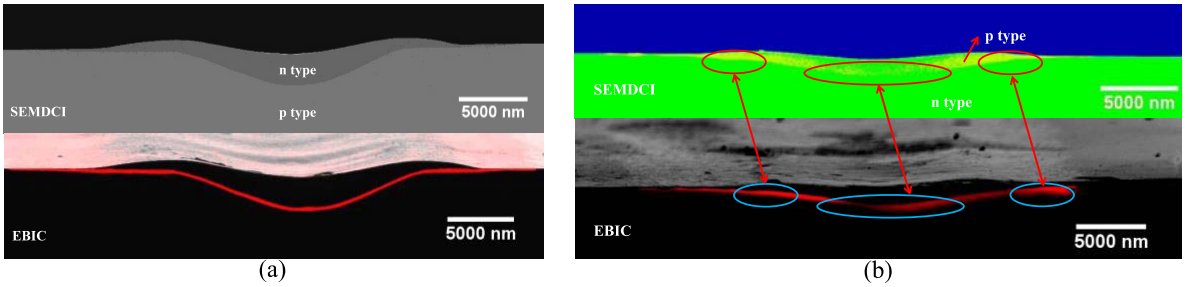

(a) (b)

Fig. 1. (a) SEMDCI and EBIC images of Sample B1. The good agreement between the two images regarding the shape of the p-n junction is evident; (2) SEMDCI and EBIC images of Sample C2.

3.3. Resolution and sensitivity

An example of the challenges associated with non-uniform and discontinuous doping distribution is presented in Fig. 2 (a). Due to the high energy pulse used for this sample, a poor electrical contact was formed. The EBIC signal was detected only from one line. Unfortunately it was not possible to characterise this line by SEMDCI. Therefore a direct comparison of the same cross-section is not available for this sample. However comparison between similar lines of the same sample still provides valuable insights. Fig. 2(a) demonstrates the ability of both SEMDCI and EBIC to image a rough, complicated, non-uniform and discontinuously doped region. Given the high spatial resolution of the EBIC technique evident in Fig. 2(a), the apparent disagreement between SEMDCI and EBIC images for some samples regarding the uniformity of doped regions, as illustrated in Fig. 2(b), is likely explained by the different sensitivity of the two techniques. In particular, the dark regions within the lightly coloured p doped regions visible in the SEMDCI image would at first glance appear to suggest that these regions are not p doped but are instead n doped with similar doping concentration to the substrate. However, contrast in SEMDCI is often only observed when the p dopant concentration exceeds a few 10^{17} cm^{-3} [4]. Thus, the darker regions may instead be lightly doped p type, an interpretation that is supported by the EBIC image. Whether this lack of contrast at low doping concentrations is significant or not will depend on the particular application, but the limitations must always be kept in mind. In addition, by inspecting the edge of the laser doped region as circled in Fig. 2(b), it can be found that the EBIC signal has a sharp top edge that basically agrees with the p-n junction location imaged by SEMDCI. However, the main part of the EBIC signal width extends into the lowly doped bulk with a blurry bottom edge. This is believed to be caused by two following reasons. Firstly, the built-in electric field of the depletion region distributes mainly within the lowly doped region, therefore resulting in more EBIC signal from the bulk. Secondly, when SEM electron beam scans to the regions where are close to but not in the depletion region, the carrier pairs generated there are possible to flow into the depletion region and be accelerated by the built-in electric field there to form a measurable current if they have long diffusion lengths. Because the lightly doped bulk normally has fewer defects compared to the highly doped laser doping region, the excess carriers generated in the bulk have longer diffusion length leading to a higher possibility to flow to depletion region and to generate EBIC signal.

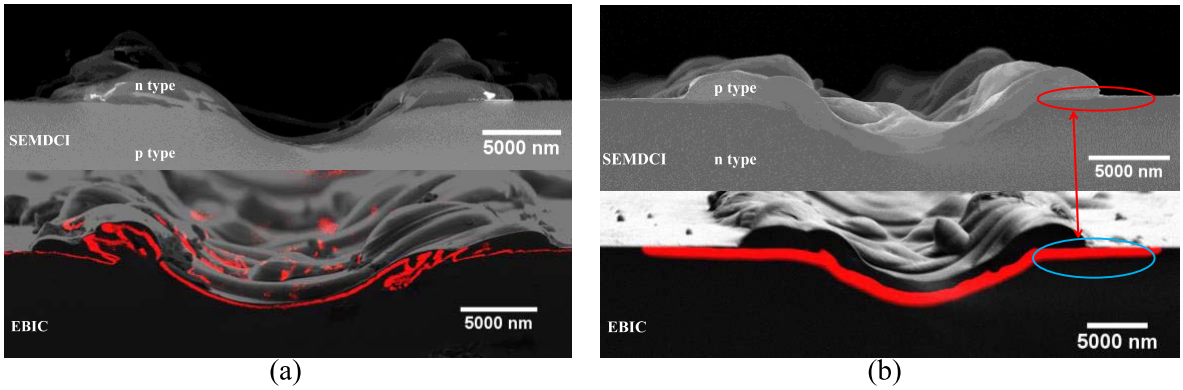

Fig. 2. (a) SEMDCI and EBIC images of Sample B3; (b) SEMDCI and EBIC images of Sample C3.

3.4. Quantitative analysis difficulty and error

As the SEMDCI and EBIC images were taken using different equipment in different institutes, there are unavoidable differences between the SEMDCI and EBIC images, for example the sample tilting angle and the pixel resolution. Therefore, a quantitative analysis is difficult. However, 1D information such as maximum doped region width can still be extracted from the images for a comparison.

Fig. 3 shows the maximum doped region widths and the dimensions of some obvious topographical features (such as the laser induced surface lump as shown in Fig. 2(b).) extracted from SEMDCI and EBIC images where the same cross-section comparison is available (note that there is no measurable topographical feature for the very smooth Samples C1 and C2). The results are shown in the form of the ratio between the EBIC and the SEMDCI data. It was found that the maximum doped region widths obtained from EBIC are wider than that of SEMDCI. This finding can be explained by system error and difference of the sensitivity. Firstly, the system error was evaluated by measurement the dimensions of some obvious topographical features. Differences were found for dimension of pure topographical features. Further investigation indicates that this disagreement is very likely caused by different working distance used for the SEMDCI and EBIC. The longer working distance which was used for EBIC might causes image distortion, especially near the image edges. It was found that this systematic error is similar for all the tested images and can be easily corrected by using a calibration constant. The modified maximum doped region width ratio after this correction is also plotted in Fig. 3. It was found that this systematic error contributes around 11% to the measured difference between SEMDCI and EBIC. Therefore the sensitivity difference between the systems can then be estimated by ~10%. It was noticed that the maximum doped region width ratio of A1 is much lower than other samples, especially compared to Sample B1. This might be due to the so called ‘depletion region effect’ [4, 8, 13-15] or due to the difference dopant distribution of the two samples. As n type and depletion regions both appear dark in SEMDCI image, if the substrate is lowly doped (such as A1), the depletion region extends mainly into the p type region so the p-n junction outline shown by SEMDCI image is deeper than the actual position. Therefore, although EBIC has higher sensitivity and usually detects a deeper/wider junction compared to SEMDCI, the effect is compensated by the depletion region effect of SEMDCI, resulting in a lower ratio value for A1. Another possible explanation is that Sample A1 may has an abrupt p-n junction with a relatively high dopant concentration close to the junction boundary, in this case the sensitivity difference of SEMDCI and EBIC has a smaller impact, resulting in a low ratio value.

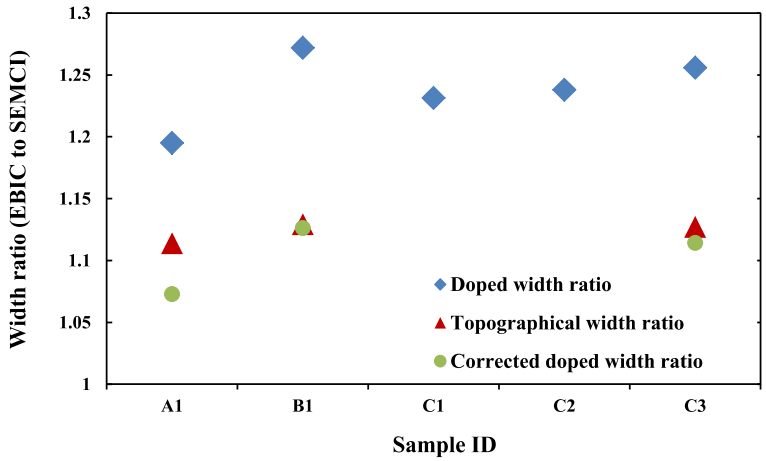

Fig. 3: A quantitative comparison between data measured by SEMDCI and EBIC including the maximum doped region width, the size of topographical features and the corrected maximum doped region width after taking into account the systematic error (see text). The results are shown in the form of a ratio between the EBIC and SEMDCI data. No obvious measurable topographical feature was found in Samples C1 and C2.

4. Conclusion

EBIC is a well-established and widely used characterisation method for laser doping to display the p-n junction position, while SEMDCI is a newly applied technique that may provide a faster, easier and cheaper measurement. The two techniques were compared qualitatively and quantitatively for laser doping applications. The good agreement demonstrated between of the two methods in terms of p-n junction shape indicates that SEMDCI can be used as a reliable technique for characterising laser doping p-n junction. Both techniques were shown to be able to detect a complicated, non-uniform and discontinuous doped region. It was found that EBIC provides a better detective sensitivity regarding the doping concentration than SEMDCI, while SEMDCI requires less and easier sample preparation and provides additional information regarding the dopant distribution. The comparison highlights the advantages and the limitations of each of the techniques, so better use of them can be done.

Acknowledgements

The authors thank Hua Chen (ANU, Australia) for helpful discussions. The Solar Energy Research Institute of Singapore (SERIS) is sponsored by the National University of Singapore (NUS) and Singapore's National Research Foundation (NRF) through the Singapore Economic Development Board (EDB). This research is partially supported by the National Research Foundation, Prime Minister's Office, Singapore under its Clean Energy Research Program Programme (CERP Award No. NRF2010EWT-CERP001-022).

References

[1] Hameiri Z, Mai L, Puzzer T, Wenham SR. Influence of laser power on the properties of laser doped solar cells. Sol Energ Mat Sol C. 2011;95(4):1085-94.
[2] Leamy HJ. Charge collection scanning electron microscopy. J Appl Phys. 1982;53(6):R51-R80.
[3] Meoded T, Shikler R, Fried N, Rosenwaks Y. Direct measurement of minority carriers diffusion length using Kelvin probe force microscopy. Appl Phys Lett. 1999;75(16):2435-7.
[4] Xu L, Weber K, Sieu Pheng P, Fell A, Brink F, Di Y, et al. Secondary electron microscopy dopant contrast image (SEMDCI) for laser doping. IEEE J Photovolt. 2013;3(2):762-8.

[5] Xu L, Weber K, Phang S, Pheng , Fell A, Brink F, Franklin E. Dopant mapping for laser doping using secondary electron image. 27th EUPVSEC. Frankfurt, Germany 2012. p. 740 - 3.
[6] Elliott SL, Broom RF, Humphreys CJ. Dopant profiling with the scanning electron microscope—A study of Si. J Appl Phys. 2002;91(11):9116-22.
[7] Castell MR, Perovic DD, Lafontaine H. Electronic contribution to secondary electron compositional contrast in the scanning electron microscope. Ultramicroscopy. 1997;69(4):279-87.
[8] Venables D, Maher DM. Quantitative two-dimensional dopant profiles obtained directly from secondary electron images. J Vac Sci Technol B Microelectron Nanometer Struct. 1996;14(1):421-5.
[9] Turan R, Perovic DD, Houghton DC. Mapping electrically active dopant profiles by field-emission scanning electron microscopy. Appl Phys Lett. 1996;69(11):1593-5.
[10] Perovic DD, Castell MR, Howie A, Lavoie C, Tiedje T, Cole JSW. Field-emission SEM imaging of compositional and doping layer semiconductor superlattices. Ultramicroscopy. 1995;58(1):104-13.
[11] Chi JY, Gatos HC. Determination of dopant-concentration diffusion length and lifetime variations in silicon by scanning electron microscopy. J Appl Phys. 1979;50(5):3433-40.
[12] de Kock AJR, Ferris SD, Kimerling LC, Leamy HJ. SEM observation of dopant striae in silicon. J Appl Phys. 1977;48(1):301-7.
[13] Venables D, Jain H, Collins DC. Secondary electron imaging as a two-dimensional dopant profiling technique: Review and update. J Vac Sci Technol B Microelectron Nanometer Struct. 1998;16(1):362-6.
[14] Buzzo M, Ciappa M, Millan J, Godignon P, Fichtner W. Two-dimensional dopant imaging of silicon carbide devices by secondary electron potential contrast. Microelectron Eng. 2007;84(3):413-8.
[15] Buzzo M, Ciappa M, Stangoni M, Fichtner W. Two-dimensional dopant profiling and imaging of 4H silicon carbide devices by secondary electron potential contrast. Microelectron Reliab. 2005;45(9–11):1499-504.
[16] Sealy CP, Castell MR, Wilshaw PR. Mechanism for secondary electron dopant contrast in the SEM. J Electron Microsc. 2000;49(2):311-21.